Journal of Pharmacy and Pharmacology 6 (2018) 305-319
doi: 10.17265/2328-2150/2018.04.002

Cytotoxic Effect of Chitosan Based Nanocomposite Synthesized by Radiation: *In Vitro* Liver and Breast Cancer Cell Line

A. Abaza[1], G. A. Mahmoud[2], E. A. Hegazy[2], M. Amin[3], E Shoukry[3] and B. Elsheikh[3]

1. Nuclear and Radiological Regulatory Authority (ENRRA), Cairo 11762, Egypt

2. National Center for Radiation Research and Technology (NCRRT), Atomic Energy Authority, Cairo 11762, Egypt

3. Faculty of Science, Al-Azhar University, Nasr City, Cairo 11371, Egypt

Abstract: A silver nanoparticle (AgNP) is likely to provide an attractive object for combining a variety of biochemical properties with great therapeutic potential by using radiation. The present study explores the IC_{50} value of chitosan-poly (vinyl alcohol) hydrogel (Cs/PVA) and Ag-doped chitosan-poly (vinyl alcohol) (Cs/PVA/Ag) nanocomposite in view of their anticancer application. The aim was to develop (Cs/PVA) based hydrogel synthesized by gamma radiation which could behave both as a nanoreactor for Ag nanoparticle with promising anticancer applications. The (Cs/PVA/Ag) nanocomposite was confirmed by FTIR (Fourier transform infrared) spectroscopy, XRD (X-ray diffraction) and EDX (energy dispersive X-ray) analysis. The anti-cancer activity of the prepared nanocomposites was demonstrated in human liver cancer cell line (HEPG2) and breast cancer cell lines (MCF7). It has significant effects against human liver cancer cell line HEPG2 compared to breast cancer cell line MCF7. Further quantitative analysis on the molecular and protein levels is still required to confirm the impact of chitosan on genotoxic effect before reaching a final conclusion and starting its biomedical application.

Key words: Chitosan, nanocomposite, silver nanoparticles, liver cancer cell line, breast cancer cell line.

1. Introduction

Hydrogel is polymeric three-dimensional network structures obtained from a source of synthetic and/or natural polymers [1]. Biocompatibility, processability and biodegradability are important parameters in hydrogel synthesis for biomedical applications. Synthesis of biocompatible hydrogel matrix from a nontoxic, economical, and easily available materials such as polysaccharides is recommended [2]. The radiation-induced synthesis of hydrogel is considered to be a promising process that can be optimized to form a sterilized gel matrix and hence can be used without further purification for various biomedical applications [3].

Corresponding author: Aya Abaza, PhD., M.D. assistant professor doctor of safety and prevention of oncology, research field: cytotoxicity of chitosan based nanocomposite and silver nanoparticles on liver and brest cancer cell line.

Fortunately, chemotherapy plays a major role in the management and treatment of cancer. However, the major drawbacks of chemotherapy are its whole-body effects, high price, and low level of efficiency [4]. Therefore, there is an urgency to develop efficient methods that minimize the side effects of chemotherapy by specifically delivering the chemotherapeutic agent to only the tumor cells [5]. Nowadays, human breast cancer is the second most common cause of cancer-related deaths in women and the incidence of breast cancer has increased worldwide in the last few years [6]. Additionally, HCC (hepatocellular carcinoma) is the most common type of cancer among the Egyptian population. It is increasing in parallel to hepatotropic viral infections and is expected to at least double in the next 20 years. There are many strategies for treating HCC but all of them are very expensive and time consuming and have several

side effects [7]. However, Chitosan possess antitumor activity tested both *in vitro* and *in vivo* [8]. *In vitro* Chitosan exerted vigorous cytotoxicity against a colon cancer cell line (Calo320), gastric cancer cell line (BGC823), and liver cancer cell line (BEL7402) and HepG2. HepG2 cells are a suitable *in vitro* model system for the study of polarized human hepatocytes. These findings suggest their application as a novel class of drugs against HCC [9]. Fortunately, Chitosan based hydrogels have been used for breast cancer, brain tumor, localized solid tumors, primary and secondary osteosarcoma, osteolysis and lung metastasis [10].

Nanomaterial-based therapeutics has recently attracted increasing attention. Metal nanoparticles including platinum, silver, copper, and gold are particularly well suited for these nanoparticle-based biological applications because of their ability to absorb and/or scatter light [11, 12]. Additionally, Silver Nanoparticles display a synergistic effect [13] and also a cytotoxic effect on cell viability which have a chief role in antitumor and anticancer effect [14, 15]. On the other hand, it can be used as antimicrobial agents in surgically implanted catheters in order to reduce the infections caused during surgery and are proposed to possess anti-fungal, anti-inflammatory, anti-angiogenic and anti-permeability activities [16-18]. However, significant new progress in the modification of nanoparticles is necessary for the further development of nanoscale components and functional materials [19].

The aim of the current work was to examine the cytotoxic effect of prepared (Cs/PVA) hydrogel and (Cs/PVA/Ag) nanocomposite that is prepared by gamma irradiation and the characterization by (FTIR), (XRD) and (EDX) analysis, in human liver cancer HEPG2 and MCF7 breast cancer cell lines.

2. Materials and Methods

2.1 Materials

Poly (vinyl alcohol) (PVA; Mw 15,000) and medium molecular weight chitosan (Cs) were purchased from Sigma-Aldrich Inc and were used as received. The other chemicals were reagent grade and used without further purification. Other chemicals were purchased from El-Nasr Co. for Chemical Industries, Egypt and used without further purification.

2.2 Methods

2.2.1 Preparation of Cs/ PVA Hydrogel

A stock solution of 1wt% chitosan (Cs) and a solution of 10 wt% polyvinyl alcohol (PVA) were prepared. Different compositions of Cs/PVA were prepared in weight ratio Cs: PVA; 1:9, 2:8, 3:7, 4:6, 5:5 and 6:4 (V/V). The solutions were poured into test tubes (inner diameter 5 mm) and subjected to gamma-irradiation at different irradiation doses; 10, 20, 25, 30, 35 and 40 kGy. Irradiation of samples was carried out using a Co^{60} gamma source installed at the NCRRT (National Centre for Radiation Research and Technology), Egypt. After irradiation the formed hydrogels were cut into nearly equal disks. The obtained hydrogels were extracted in distilled water at room temperature over night to remove the non-cross-linked polymer, and then dried in air to constant weight.

2.2.2 Preparation of Cs/PVA/Ag Nanocomposites

A 0.1 g of dried Cs/PVA hydrogel (Cs: PVA; 1: 9) was placed in 50 mL of Ag ion solution of concentration 250 mg/L for 24 h to dope the Ag ions in the hydrogel matrix. Ag ion loaded hydrogels were placed in distilled water for another 24 h to remove unbound metal ions. The Ag ions inside the hydrogels were reduced by transferring them into 50 mL of 5% NaOH for 6 h and then in 50 mL of 0.5 M $NaBH_4$ for another 6 h to complete reduction of Ag. Soaking them in de-ionized water for 12 h and drying in oven at 40^{o}C.

2.2.3 Gel Content

To determine the insoluble part in the hydrogel, the hydrogel samples were air-dried to a constant weight. The dried samples were soaked in distilled water for 24 h at 80 ^{o}C then taken out and washed with hot water to

remove the soluble part and dried to a constant weight. The gel content was calculated gravimetrically applying the following formula:

$$\text{Gel content (\%)} = \frac{W_d}{W_0} \text{ X } 100 \qquad (1)$$

where W_d and W_0 are the dried sample weights after and before extraction, respectively.

2.2.4 Instrumentations

The functional groups of the synthesized systems were characterized by FTIR; Nicolet IS-10 FTIR, in the range 400-4,000 cm-1 using KBr pellets.

EDX analysis was carried out during the surface analysis done by scanning electron microscopy (JSM-5400, JEOL).

The diffraction patterns of the crystal structure were analyzed XD-DI Series, Shimadzu apparatus using nickel-filtered and Cu-K target.

TEM (transmission electron microscope) measurements were performed using TEM JEOL: JEM-100cx.

2.3 Human Tumor Cell Lines

Human tumor carcinoma liver HepG2 and breast MCF7 cell lines used in this study were obtained from the American Type Culture Collection (ATCC, Minisota, U.S.A.). The tumor cell lines were maintained at the National Cancer Institute, Cairo, Egypt, by serial sub-culturing. Samples were prepared by dissolving 1:1 stock solution and stored at -20 ^{o}C in dimethylsulfoxide (DMSO) at 100 mM. Different concentrations of the drug were used 5, 12.5, 25, 50 µg/mL.

2.3.1 Cell Culture and Maintenance

RPMI-1640 medium was used for culturing and maintenance of the human tumor cell lines. The medium was supplied in a powder form. The working solution was prepared by dissolving 10.4 gm powder and 2 gm sodium bicarbonate dissolved in 1 L distilled water. The medium was then sterilized by filtration in a Millipore bacterial filter (0.22 µm). The prepared medium was kept in a refrigerator (4 ^{o}C). Before use the medium was warmed at 37 ^{o}C in a water bath and the supplemented with 1% penicillin/streptomycin and 10% fetal bovine serum. A cryotube containing frozen cells was taken out of the liquid nitrogen container and then thawed in a water bath at 37 ^{o}C. Then the cryotube was opened under strict aseptic conditions and its contents were supplied by 5 mL supplemented medium drop by drop in a 50 mL sterile falcon tubes. The tube was incubated for 2 hours then centrifuged at 1,200 rpm for 10 minutes and the supernatant was discarded, the cell pellet was suspended and Seeded in 5 mL supplemented medium in T25 Nunclon sterile tissue culture flasks. The cell suspension was incubated and followed up daily the supplemented medium was replaced every 2-3 days. Incubation was continued until a confluent growth was achieved and the cells were freshly subcultured before each experiment to be in the exponential phase of growth.

2.3.2 *In Vitro* Cytotoxic Assay for HepG2 and MCF7 Cancer Cell

The cytotoxicity was carried out using SRB (sulphorhodamine-B) assay following the method reported by Vicha and Kirtikara [20]. SRB is a bright pink aminoxanthrene dye with two sulphonic groups. It is a protein stain that binds to the amino groups of intracellular proteins under mildly acidic conditions to provide a sensitive index of cellular protein content. Cells were seeded in 96-well microtiter plates at initial concentration of 3×10^3 cell/well in a 150 µL fresh medium and left for 24 hours to attach to the plates. Different concentrations 0, 5, 12.5, 25, 50 µg/mL of drug were added. For each drug concentration, 3 wells were used. The plates were incubated for 48 hours. The cells were fixed with 50 µL cold trichloroacetic acid 10% final concentration for 1 hour at 4 ^{o}C. The plates were washed with distilled water using (automatic washer Tecan, Germany) and stained with 50 µL 0.4% SRB dissolved in 1% acetic acid for 30 minutes at room temperature. The plates were washed with 1% acetic acid and air-dried. The dye was solubilized with 100 µL/well of 1.0 M tris base (pH 10.5) and optical density

(O.D.) of each well was measured spectrophotometrically at 570 nm with an ELISA microplate reader (Sunrise Tecan reader, Germany). The mean background absorbance was automatically subtracted and means values of each drug concentration was calculated. The experiment was repeated 3 times. The percentage of cell survival was calculated as follows:

Surviving fraction = O.D. (treated cells)/ O.D. (control cells).

The IC50 values (the concentrations of resveratrol required to produce 50% inhibition of cell growth) were also calculated.

3. Result and Discussion

The variation of gel fraction of Cs/PVA hydrogel as a function of the copolymer composition at various irradiation doses is shown in Fig. 1. It was observed that the gel fraction increased with increasing PVA content in the hydrogel or decreased with increasing chitosan content. The higher the Cs content the lower the gel fraction was obtained. In other meaning, the lower the cross-linking density has obtained the presence of more Cs content. The same behavior was observed in other studies [21, 22]. It is well known that PVA is a cross-linking type polymer and chitosan as a polysaccharide is more likely to degrade when exposed to gamma radiation. When Cs/PVA solution mixture is exposed to gamma irradiation, cross-linking of PVA and degradation of Cs to shorter chains takes place simultaneously. At the same time occurs to the formation of a three-dimensional network of hydrogel structure. The mechanism of crosslinking involves the cleavage of C-H bonds in neighboring polymer chains, subsequently; the polymeric radicals recombine to form intermolecular bonds. It is well known that in aqueous solution, the indirect effect of radiation is the main interaction mode, i.e. the primary reactions occur with water, producing powerful oxidizing species, such as hydroxyl radicals OH, that can attack the glycosidic bonds of chitosan. Hence, the radiation processing of chitosan in presence of water would reduce significantly

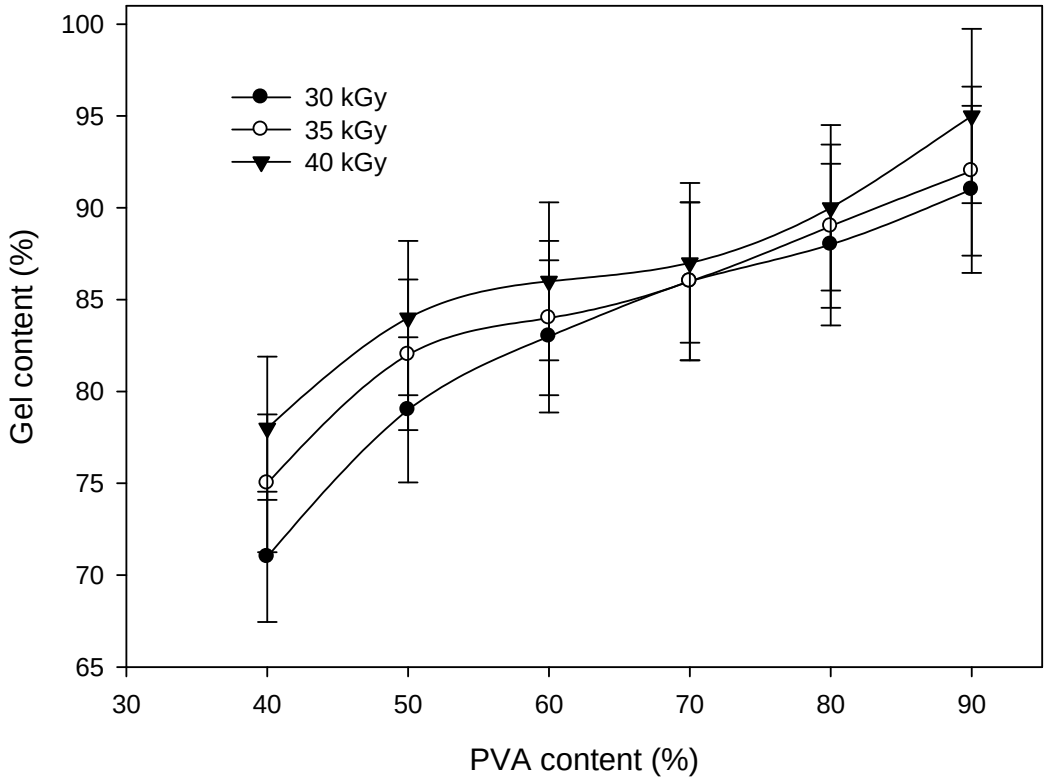

Fig. 1 Effect of PVA content on the gel content at different irradiation doses.

its molecular weight. It was reported that, when an aqueous solution of PVA containing polysaccharides is exposed to radiation, OH, H radicals and hydrated electrons are produced, as a major part of the energy is absorbed by the solvent. OH radicals are mostly responsible for crosslinking of PVA and degradation of polysaccharides, and the rates of OH radical reaction with PVA and polysaccharides are similar. Therefore, besides crosslinking of PVA, a fraction of radicals would also degrade the polysaccharides in proportion to their concentration in aqueous PVA solution [23].

It must be known that Cs in the Cs/PVA hydrogel controls its flexibility. The cross-linking strength of Cs is weaker than that of PVA, even if Cs formed a cross-linking structure with PVA in the hydrogel. Generally, as the strength of the gel is weakened the flexibility is strengthened [24]. This means Cs is used in the hydrogel to control the biocompatibility and flexibility which are important in biomedical applications. As seen in Fig. 1, the gel fraction increases with increasing the irradiation dose at the same copolymer composition. The increase in the total irradiation dose enhances the formation of radicals in the reaction mixture which causes a high degree of crosslinking and thus a high gel fraction. The highest obtained gel fraction was at irradiation dose 40 kGy and copolymer composition (1:9) (Cs: PVA).

The in situ preparation of Ag nanoparticle in the hydrogel was done and the mechanism of preparation is shown in Fig. 2. The hydrogel networks act as a template for in situ deposition of Ag nanoparticles. The Ag^+ were loaded into the hydrogel network and oxidized by NaOH and $NaBH_4$ as oxidizing agents. This technique has been used in many studies because of being facile and not required heat or any other tools for nanoparticle synthesis [25].

3.1 FTIR (Fourier Transform Infrared Spectroscopy)

The FTIR spectra of Cs/PVA and Cs/PVA/Ag were evaluated as shown in Fig. 3. The synthesized hydrogels displayed good compatibility between Cs and PVA polymer with significant changes observed

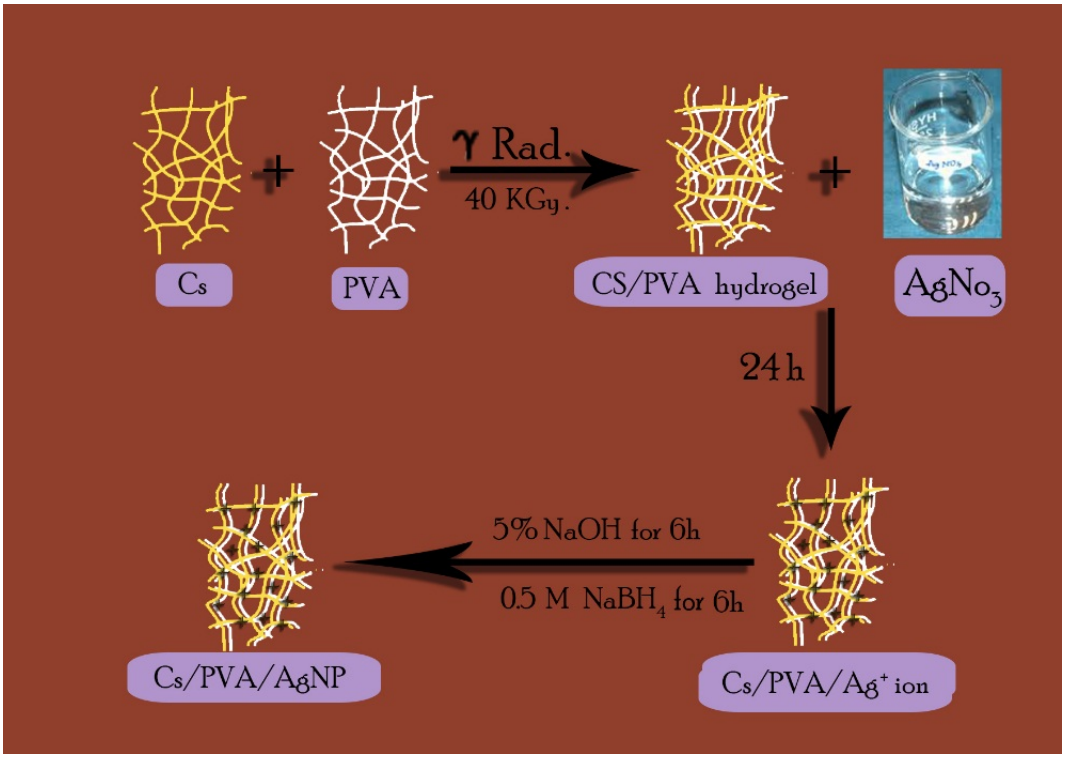

Fig. 2 Proposed scheme for preparation of Cs/PVA/Ag nanocomposites.

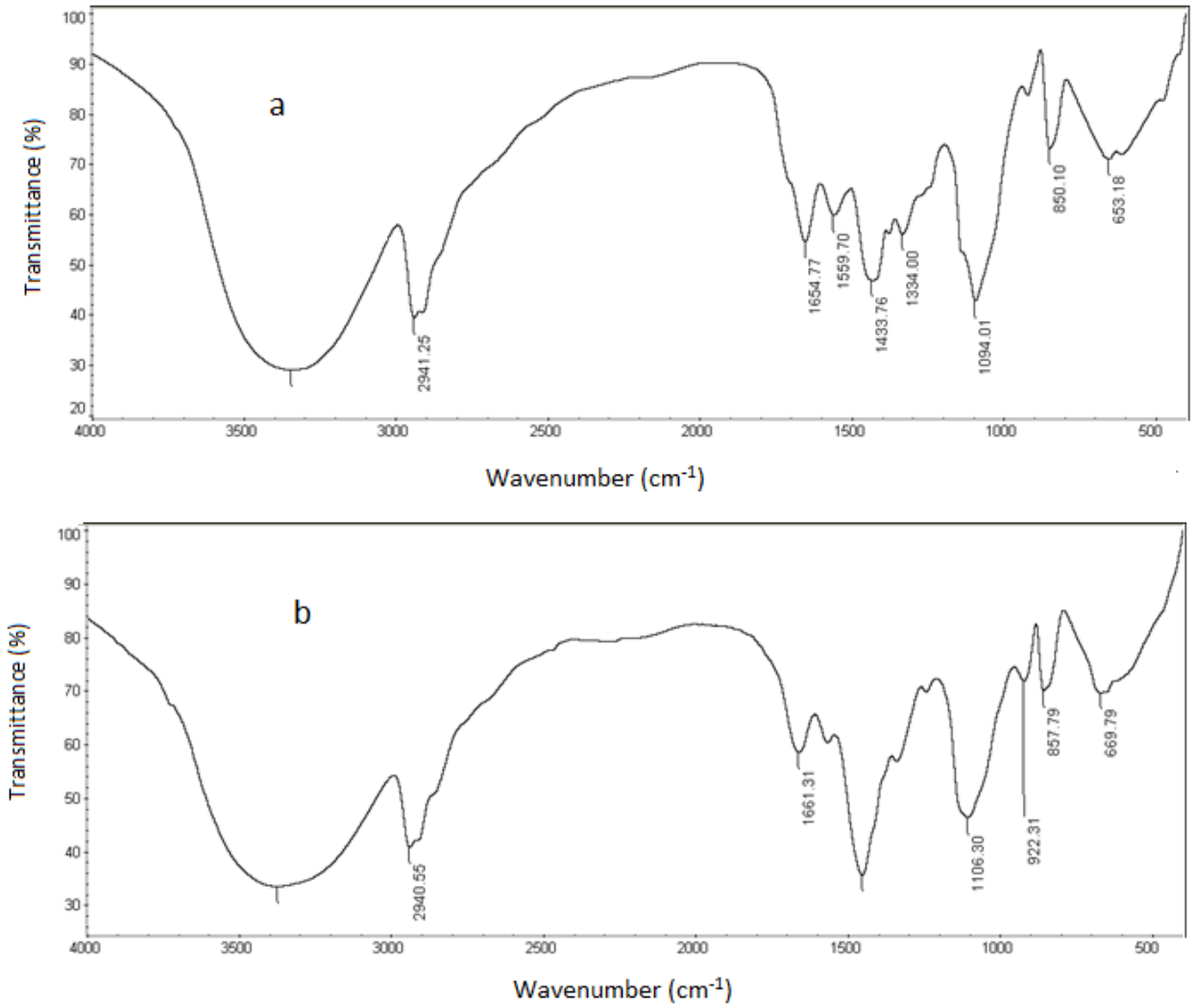

Fig. 3 FTIR spectra of Cs/PVA (a) and Cs/PVA/Ag(b).

after metal nanoparticle incorporation. A peak appeared at 3,345 cm^{-1} indicates the presence of hydrogen bonds between chitosan and PVA polymers causing OH/NH_2 stretching [26]. The broad peak at 1,094 cm^{-1} indicates the C-O stretching vibration in chitosan [27]. The absorption peaks at 1,654 cm^{-1} and 1,334 cm^{-1} relating to amide I and III of C=O stretching, N-H/C-N stretching and CH_2 wagging coupled with OH groups of chitosan respectively. The peak observed at 1,447 cm^{-1} is due to CH_2 bending, and the peak at 2,941 cm^{-1} is characteristic of $-CH_2$ asymmetric stretching of Cs/PVA. The Cs/PVA/Ag (Fig. 3b) has shown all the above characteristic peaks with a slight shift of the peak 1,334 to 1,434 cm^{-1} corresponding to amide III band. In addition, the stretching vibration at 3,414 cm^{-1} corresponding to OH/NH_2 groups has shifted to 3,423 cm^{-1}, indicating that the silver particles are bounded to the functional groups present both in Cs and PVA. The shift of the peak due to formation of electrostatic attraction between the Ag and the electron rich groups present in Cs and PVA.

3.2 XRD (X-Ray Diffraction)

XRD diffractograms of Cs/PVA and Cs/PVA/Ag nanocomposite are shown in Fig. 4. The diffractogram of Cs/PVA hydrogel is characterized by a peak at 2-theta = 19.5°, which corresponds to the amorphous phase. The XRD pattern of Cs/PVA/Ag showed a decreasing in the amorphous phase and new peaks were observed. These peaks were observed at 37.8°, 43.3°

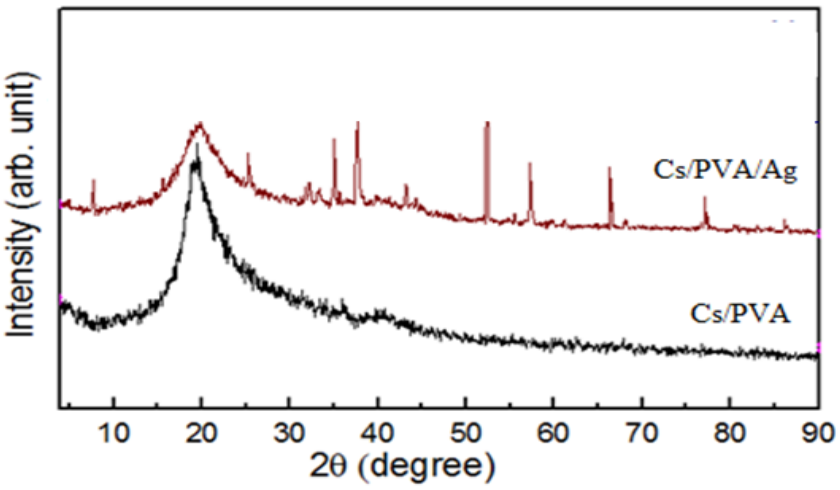

Fig. 4 XRD patterns of Cs/PVA and Cs/PVA/Ag.

and 63.5° corresponding to the crystallographic planes (111), (200), and (220) of Ag, respectively. By using the Scherrer equation, the average size of the Ag nanoparticles of the Cs/PVA/AgNP composite was estimated to be 67 nm. The Ag particle size is calculated using FWHM according to the Scherrer equation [28]. TEM micrograph of Cs/PVA/Ag is shown in Fig. 5. As seen dark small spherical particles are randomly distributed in the micrograph that confirmed the formation of Ag nanoparticles.

3.3 EDX (Energy Dispersive X-Ray)

EDX is used to estimate and quantify the amount of metals doped in the network structure. In this respect Cs/PVA of different compositions doped with Ag nanoparticles were examined and shown in (Fig. 6) respectively, where the amounts of different nano-particles estimated in Cs/PVA/AgNP gave 0.87%, 0.41% and 0.44% of Cs/PVA (1:9), (2:8) and (4:6) respectively.

3.4 Cytotoxicity Assay HepG2 and MCF7 Cells

Chitosan is inexpensive and thus is considered as potential drug carriers with great efficiency in controlled drug release [29]. On the other hand, it has been reported that the soluble Cs and Cs microspheres show some degree of toxicity towards certain cell lines like the murine melanoma cell line and the human gastric carcinoma MGC803 cell line suggesting their application as antitumor drugs [13]. Therefore, in the present study, the toxic effect against human liver cancer cells and Breast cancer cells of the prepared Cs/PVA hydrogels were evaluated to explore their possible application as an anti-cancerous drug. The HepG2 and MCF7 cell lines were used as a model for human liver cancer and breast cancer cell respectively. On the other hand, Silver nanoparticles (AgNPs) have many biomedical applications due to its excellent biocompatibility and antibacterial properties. AgNPs display a synergistic effect [15] and a cytotoxic effect on cell viability which have a principal role in antitumor effect [30, 31]. Additionally, AgNPs aid in gathering and transporting drugs into the cancer cells, [15] and they also obstruct with metabolism of cancer and tumor proliferation [32,33]. So, by using AgNP with chemotherapeutic drug, the required amount of drug will be reduced, which may lead to decreasing the side effects of the chemotherapeutic drug [34].

The cytotoxic effect of various concentrations of Cs/PVA hydrogels and Cs/PVA/Ag nanocomposites (5, 12.5, 25 and 50 μg/mL) was assessed in HepG2 cell cultures using SRB colorimetric assay at 48 h time intervals as shown in Fig. 7 and Table 1. In case of Cs/PVA hydrogel (5:5), the results showed that 12.5 μg/mL killed 34% of the cells**,** and IC_{50} reached at 21.6 μg/mL, whereas Cs/PVA hydrogel (1:9) and (4:6)

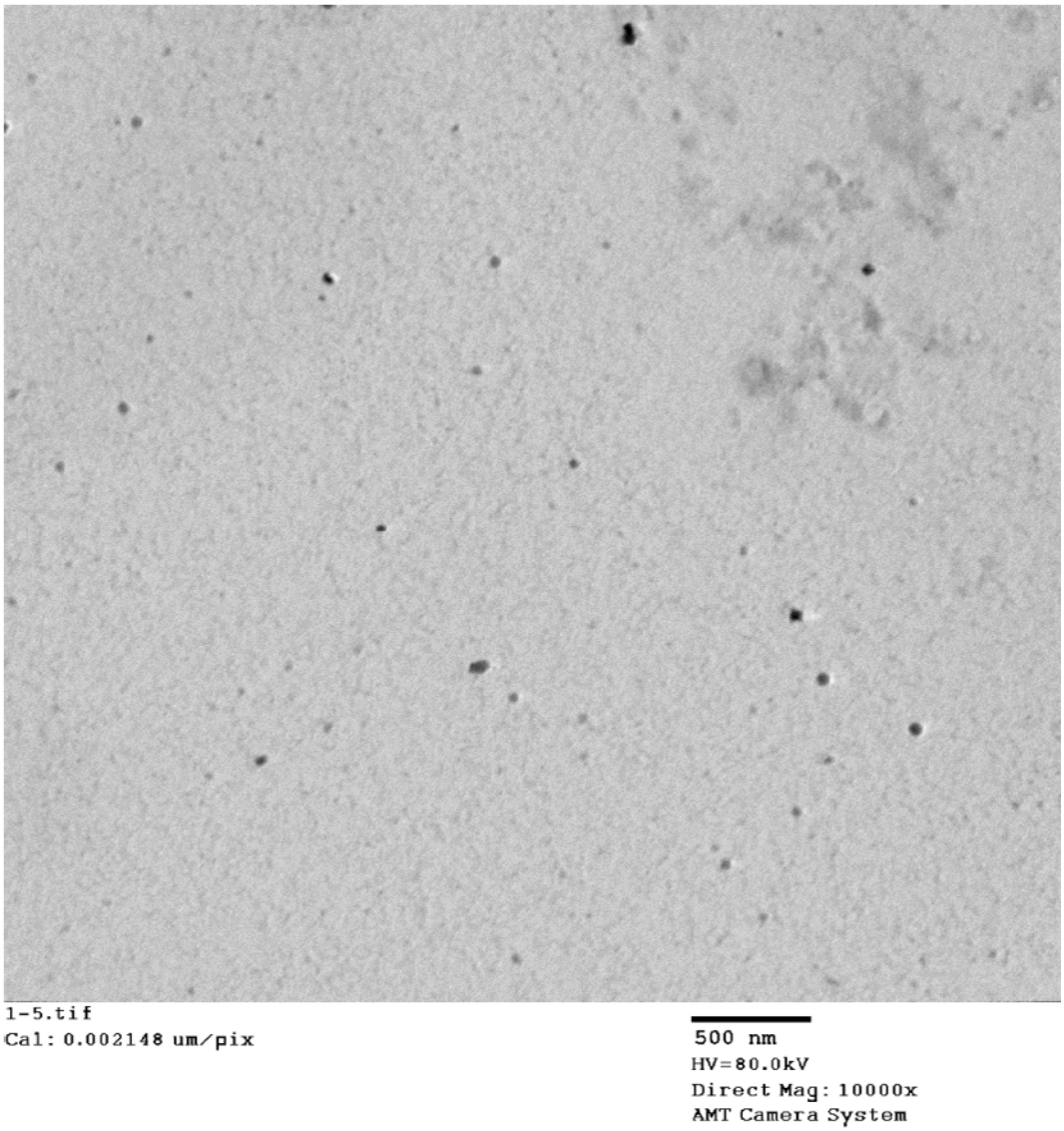

Fig. 5 TEM micrograph of Cs/PVA/Ag.

killed 29.8% and 43.9% respectively at 50 μg/mL. The inhibition of cell proliferation of Cs/PVA hydrogel was found to be increased with increasing chitosan content in the hydrogel at the culture medium, so the cell viability of the Cs/PVA hydrogel indicated that the toxicity of Cs/PVA hydrogel (1:9) is relatively small and Cs/PVA hydrogel (5:5) inhibited the cell proliferation better than Cs/PVA hydrogel (1:9) and (4:6) (Fig. 7). These differences were statistically significant. This percent is more than that reached by Loutfy et al. [9] who did not reveal any morphological alteration after 24 h and 48 h with the treatment of HepG2 with CS-NPs at 100 μg/mL and kills only 12% of the cells after 48 h of cell exposure. The inhibition rate increased with increasing Cs concentration in the culture medium, where IC_{50} was found to reach 230 μg/mL in his study. This indicated that the inhibition of cell viability by Cs-NPs was clearly dose- and time dependent. This was different when using the MGC803 human gastric carcinoma cell line where the IC_{50} value was 16.2 and 5.3 μg/mL after 24 h and 48 h, respectively, in incubation with Cs, the type of biologically interacting cells and cellular uptake dramatically affect the cytotoxic effect of Cs-NPs [9].

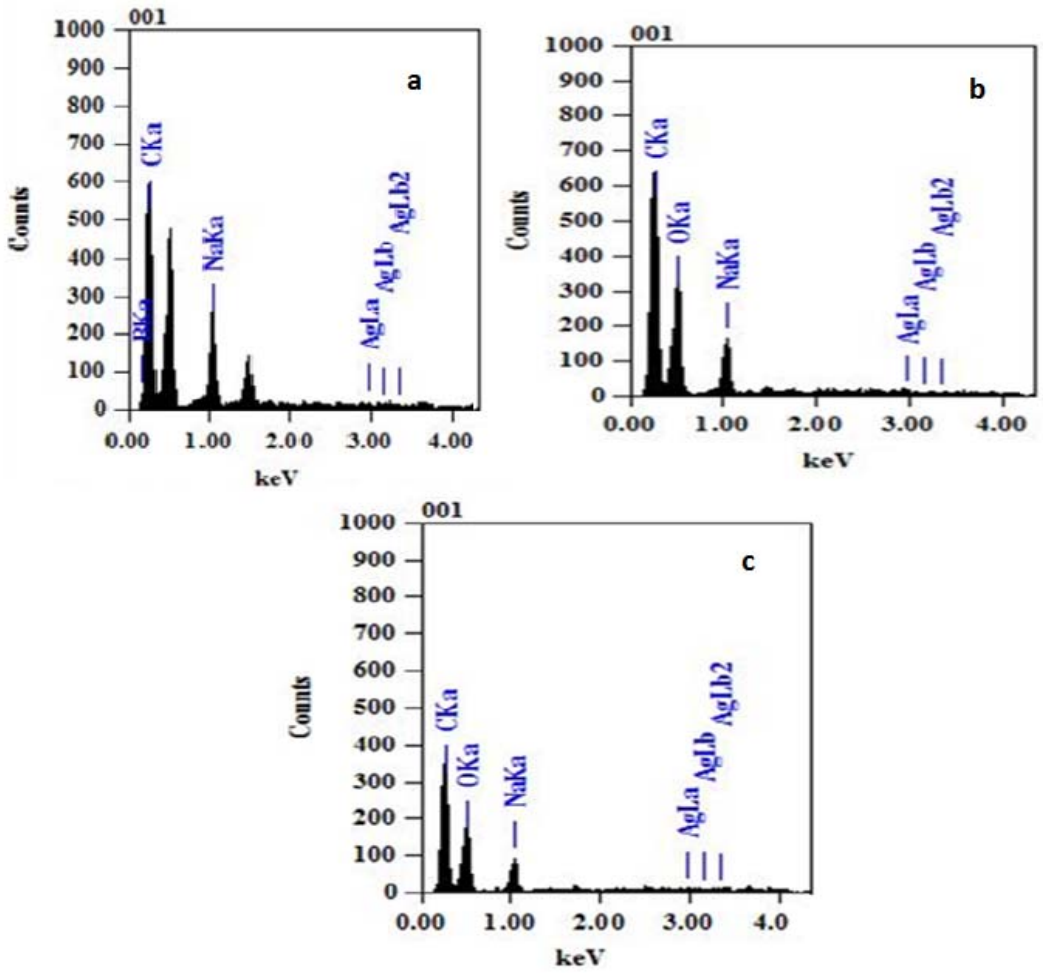

Fig. 6 EDX micrographs of Cs/PVA/Ag of different Cs: PVA compostions (a) 1:9 (b) 2:8 (c) 4:6.

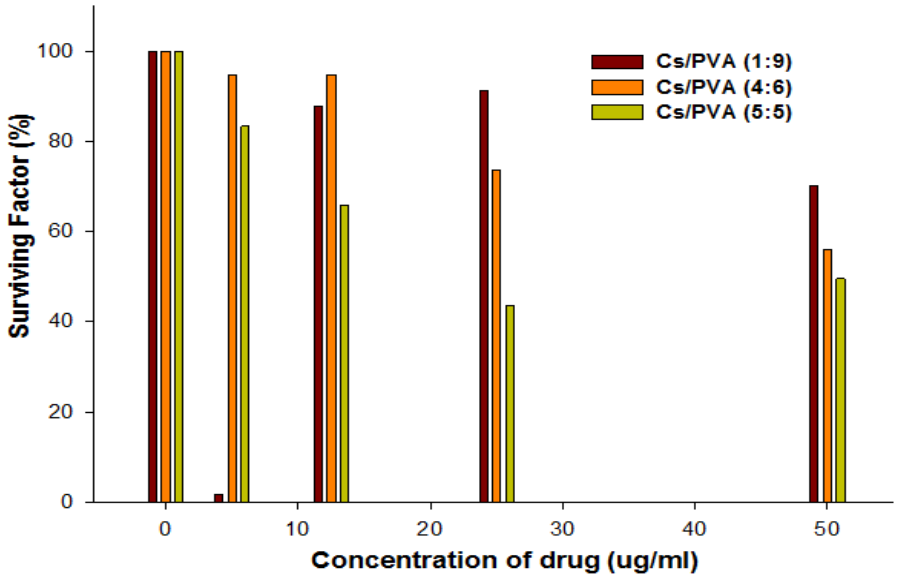

Fig. 7 Surviving factor (%) of HepG2 cells after 48 h of treatment with different Cs/PVA hydrogels, as calculated from the SRB assay.

Table 1 The percentage of inhibiting fraction at 50 ug/mL and IC_{50} values of Cs/PVA hydrogels and Cs/PVA/Ag nanocomposites on the liver cancer cell line (HepG2) using SRB colorimetric assay at 48 h time intervals.

Sample code	Inhibiting fraction (%)	IC_{50} (μg/mL)
Cs/PVA (1:9)	29.8	None
Cs/PVA (4:6)	43.9	None
Cs/PVA (5:5)	56.4	21.6
Cs/PVA/Ag (1:9)	40.8	None
Cs/PVA/Ag (4:6)	54.4	43.7

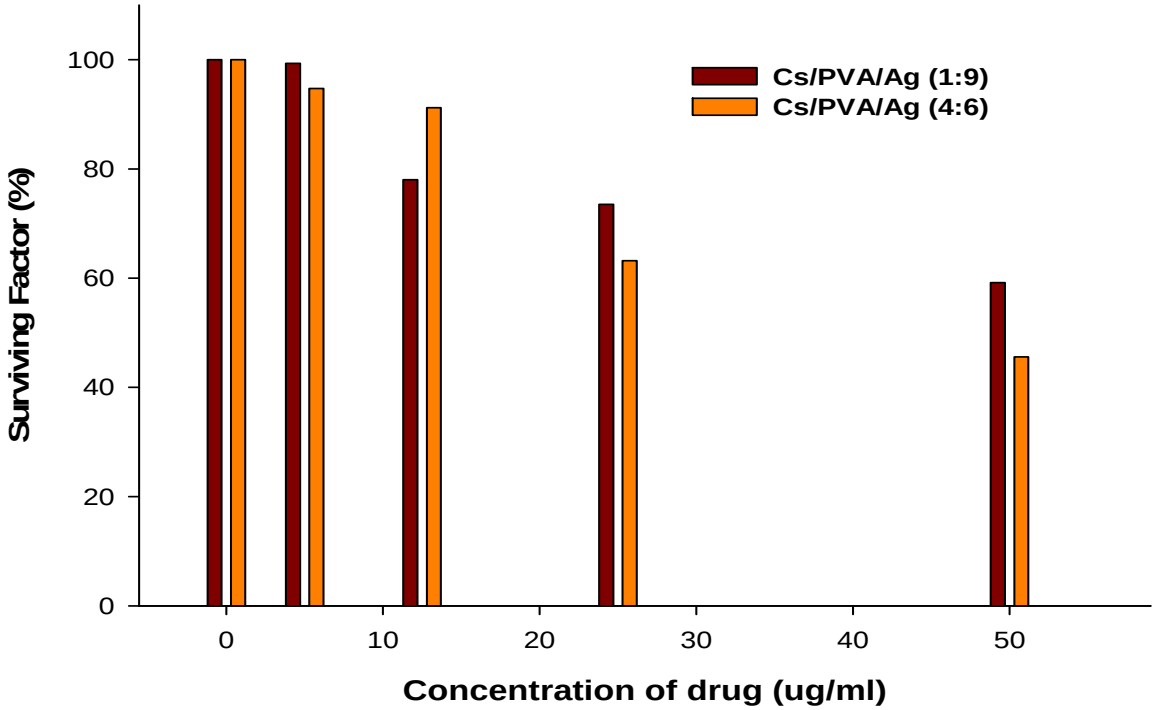

Fig. 8 Surviving factor (%) of HepG2 cells after 48 h of treatment with different Cs/PVA/Ag nanocomposites, as calculated from the SRB assay.

However, Ag nanoparticles (AgNP) loaded in Cs/PVA hydrogel, Cs/PVA/Ag (1:9) killed 40.8%, (4:6) killed 54.4%, wherefores IC_{50} reached at 43.7 μg/mL as shown in Fig. 8. Previous *in vitro* studies revealed that AgNP could cause a strong cytotoxicity in a broad spectrum of cells, such as mesenchymal stem cells, HepG2 human hepatoma cells, human glioma cells (U251), human normal bronchial epithelial (BEAS-2B) cells, and HeLa cells. These studies summarized that AgNP induced oxidative stress (OS) and apoptosis in cultured cells and animal tissues [35-37]. Contrary, Mansour et al. [32] observed that no cytotoxic activity against HepG2 cell lines. But, the combination of Doxorubicin drug and AgNPs (DOX-AgNPs) exhibits a cytotoxic effect against HepG2, cells over that of DOX alone. The IC_{50} values were 4.73, 4.13, and 4.43 mg/mL, respectively. So, the combination of AgNPs and DOX was found to be more effective than the activity of DOX individually. The NP may affect the factors that control biokinetics, DNA synthesis, or cell growth. AgNPs may have damaged the cell membrane leading to disruption in permeability that may have elevated the uptake of the drug into cells. By using AgNPs and the drugs in combination, the required amount of drug will be reduced, which may lead to a decrease in the side effects of the chemotherapeutic [33, 34]. Another study explained the exact molecular effects of AgNPs on hepatocellular carcinoma cells.

Their obtained data clarified the potentialities of the newly green synthesized NPs against hepatocellular carcinoma via mitochondrial intrinsic apoptotic pathway by upregulation of the expression of p53 and downregulation of the expression on Bcl2 gene [38]. Actually, NP can damage different organs and tissues as they are small enough to pass from smallest capillary vessel of body and biological membranes and be toxic through producing OS (oxidative stress) and free radicals [39]. The AgNPs can induce cell death *in vitro* and *in vivo* through a reactive oxygen species (ROS)-mediated apoptotic process [30, 31, 33]. However, the AgNPs exposure could induce the changes in cell shape, reduce cell viability, increase LDH release, and finally resulted in the cell apoptosis and necrosis [40]. Moreover, internalized AgNPs can disrupt the integrity of the cell membrane, cause lysosomal swelling, and even rupture lysosomal membranes [41, 33].

Regarding the cytotoxic effect of various concentrations of Cs/PVA hydrogel, and Cs/PVA/AgNp (5, 12.5, 25, 50 and 100 μg/mL) that assessed on breast cancer cells (MCF7 cell line) in the current study, the results of Cs/PVA hydrogel (5:5) and (4:6) were observed after 24 and 48 h incubation and showed that IC50 was reached at 59.8 and 69.2 μg/mL respectively, whereas Cs/PVA hydrogel (1:9) killed 49% at 100 μg/mL. However, silver nanoparticle loaded at Cs/PVA hydrogel, Cs/PVA/AgNP (1:9) killed 62%, (4:6) killed 80%, wherefore IC50 reached at 60 and 52.5 μg/mL respectively as shown in Figs. 9 and 10 and Table 2. But these differences were not statistically significant. Contrary, Manivasagan et al. [5] examined the cytotoxicity of Cs-PPy NCs for MDA-MB-231 cells using the standard MTT assay. He found that the cell viability was slightly reduced in a dose-and time-dependent manner, but no significant cytotoxicity was observed after 24 and 48 h incubation with any concentration of Cs-PPy NCs. Even after 48 h exposure to the highest concentration of Cs-PPy NCs (500 μg/mL), the viability of the cell population was more than 60%, indicating a very low cytotoxicity and a good biocompatibility for the Cs-PPy NCs. Biocompatibility of nanomaterials has been considered

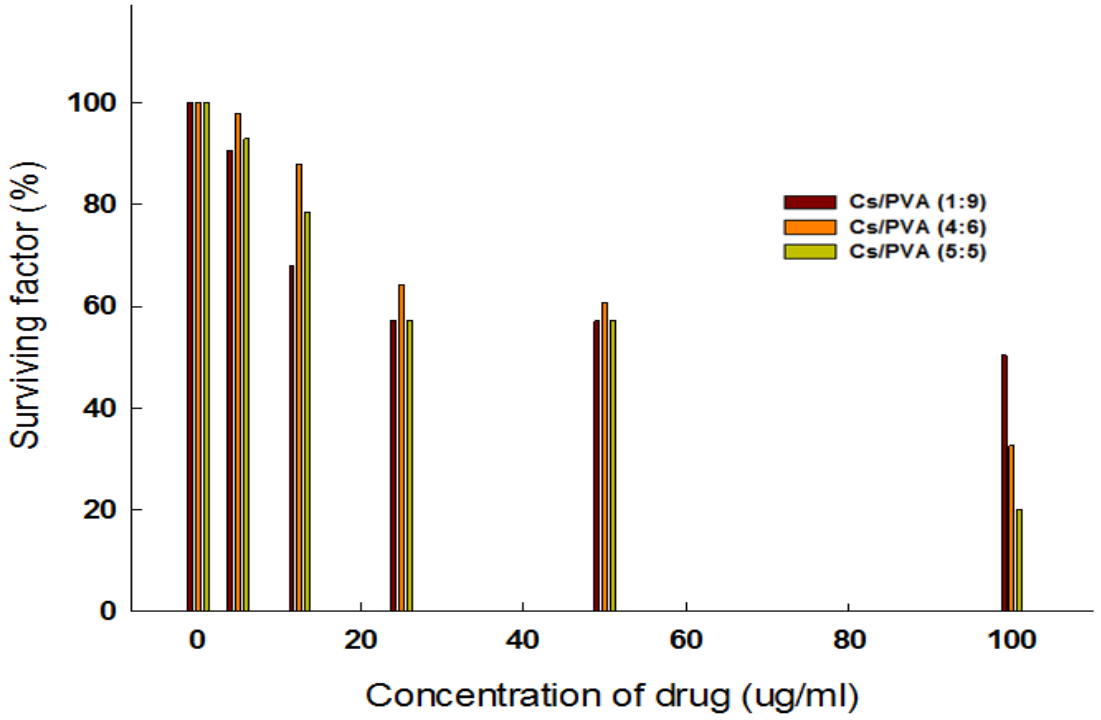

Fig. 9 Surviving factor (%) of MCF7 cells after 48 h of treatment with different Cs/PVA hydrogels, as calculated from the SRB assay.

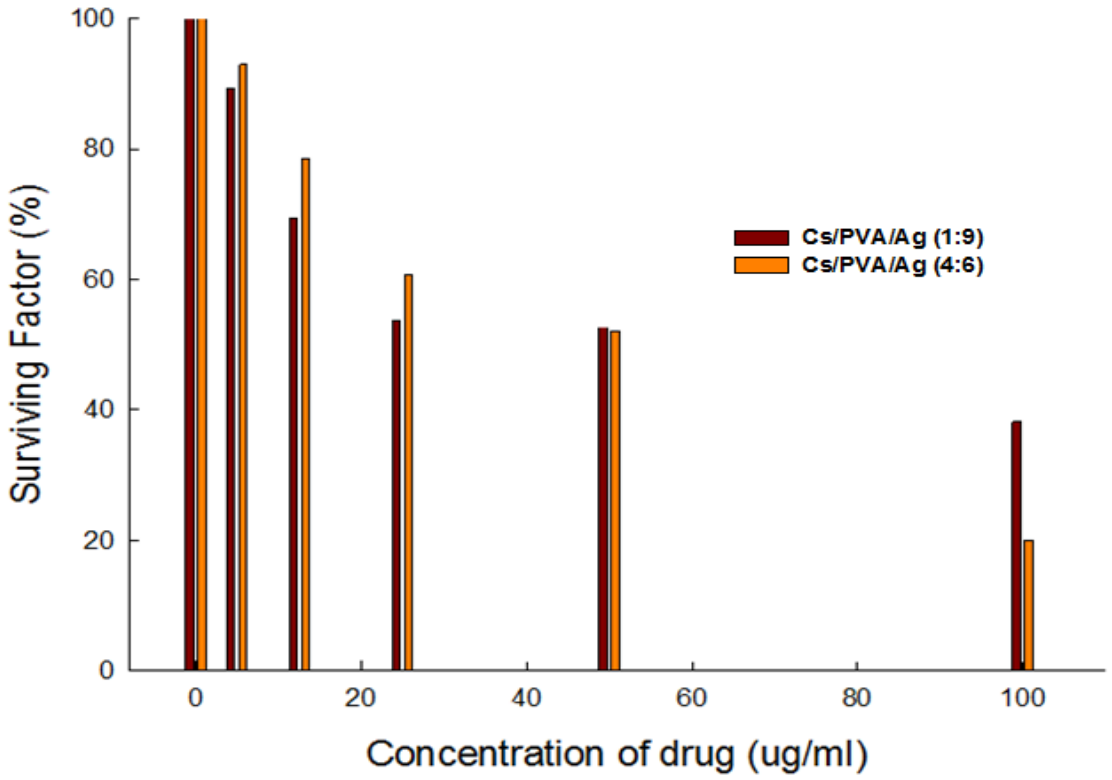

Fig. 10 Surviving factor (%) of MCF7 cells after 48 h of treatment with different Cs/PVA/Ag nanocomposites, as calculated from the SRB assay.

Table 2 The percentage of inhibiting fraction at 100 ug/mL and IC_{50} values of Cs/PVA hydrogels and Cs/PVA/Ag nanocomposites on breast cancer cell line (MCF7) using SRB colorimetric assay at 48 h time intervals.

Sample code	Inhibiting fraction (%)	IC_{50} (μg/mL)
Cs/PVA (1:9)	49.7	None
Cs/PVA (4:6)	67.4	69.2
Cs/PVA (5:5)	80	59.8
Cs/PVA/Ag (1:9)	61.8	60.0
Cs/PVA/Ag (4:6)	80	52.5

to be essential for their biomedical applications. The biocompatibility test was conducted for 24 h and 48 h on HEK 293 cells in the concentration range from 30-510 μg/mL in his study. His results showed that CS-PPy NCs are non-toxic and have excellent biocompatibility, suggesting their suitability for *in vivo* studies.

However, Chen el al. [41] did not show a considerable cytotoxicity against the MCF-7 cell line at all experimental concentrations (1.8 to 90 μg/mL) using Chitosan nanoparticles (CSNCs). The cytotoxicity enhanced by using Dox-CSNC in comparison to free Dox. Although CSNCs have no considerable cytotoxicity, Dox can be effectively delivered to MCF-7 cancer cells by using CSNCs as delivery scaffolds, resulting in enhanced cytotoxicity. The expected mechanism of AgNP induced toxicity being in the interactions between nanomaterials and cells, the cellular uptake, and subsequent toxic response of the cell are among the most crucial issues relating to AgNP-induced toxicity. For most cells, uptake of AgNPs mainly through endocytosis depends on time, dose, and energy [42]. Recent studies also indicated that, Ag can directly lead to DNA damage in addition to damaging mitochondria and inducing ROS production [43]. Furthermore, damage to mitochondria

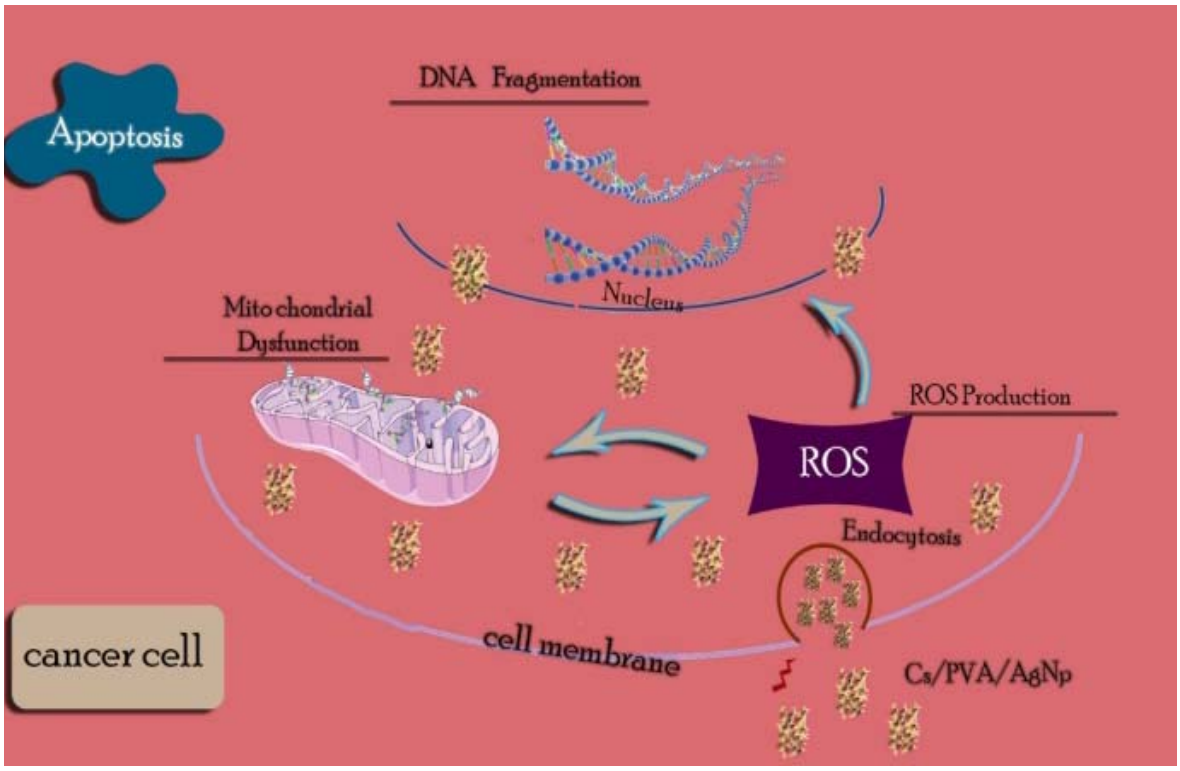

Fig. 11 Illustrative representation of the possible mechanism of Cs/PVA/Ag nanocomposite against cancer cells.

impairs electron transfer, thereby activating mitochondrion-dependent apoptosis. In addition, AgNP could readily diffuse into, and translocate to, the nucleus through nuclear pore complexes, thereby leading to the formation of ROS, which directly trigger DNA damage and chromosomal abnormalities. AgNPs and released Ag^+ prefer to interact with the thiol groups of molecules present in the cytoplasm, cell membrane, and inner membrane of mitochondria, which might release lipid peroxide and increase permeation of the cell membrane and mitochondrial systems. Damage to the cell membrane can result in leakage of cytoplasmic contents [42]. The illustrative representation of the possible mechanism of Cs/PVA/Ag nanocomposite against cancer cells is shown in Fig. 11.

4. Conclusions

The radiation-induced synthesis of hydrogel is considered to be a promising process that can be optimized to form a sterilized hydrogel matrix and hence can be used without further purification for various biomedical applications. In this study different compositions of Cs/PVA hydrogel were successfully performed by gamma radiation and were used for the in situ preparation of Ag nanoparticles to form Cs/PVA/Ag nanocomposite. The prepared hydrogel and nanocomposite were characterized by FTIR, XRD, and EDX. *In vitro* Cs/PVA hydrogel and Cs/PVA/Ag nanocomposite exerted cytotoxicity against a liver cancer (HepG2) and breast cancer (MCF7) cell lines. The antitumor activity of Cs/PVA/Ag nanocomposite was higher than Cs/PVA hydrogel in both cell lines. Silver (Ag) nanoparticles and Ag ions are known to have higher antitumor ability. Further quantitative analysis on the molecular and protein levels is still required to confirm the impact of Cs on genotoxic effect before reaching a final conclusion and starting its biomedical application.

References

[1] Mahmoud, G. A., Abdel-Aal, S. E., Badway, N. A., Elbayaa, A. A., and Ahmed, D. F. 2017. "A Novel Hydrogel Based on Agricultural Waste for Removal of

Hazardous Dyes from Aqueous Solution and Reuse Process in a Secondary Adsorption". *Polym. Bull.* 74: 337-58.

[2] Juby, K., Dwivedi, C., Kumar, M., Kota, S., Misra, H., and Bajaj, P. 2012. "Silver Nanoparticle-Loaded PVA/Gum Acacia Hydrogel: Synthesis, Characterization and Antibacterial Study." *Carbohydr. Polym.* 89 (3): 906-13.

[3] Abou Taleb, M., Hegazy, D. E., and Mahmoud, G. A. 2014. "Characterization and In-vitro Drug Release Behavior of (2-hydroxyethyl methacrylate)- co- (2-acrylamido- 2-methyl- 1- propanesulfonic Acid) Crosslinked Hydrogels Prepared by Ionizing Radiation." *Int. J. Polym. Mater.* 63: 840-5.

[4] Wang, S., Dai, Z., Ke, H., Qu, E., Qi, X., Zhang, K., and Wang, J. 2014. "Contrast Ultrasound-Guided Photothermal Therapy Using Gold Nanoshelled Microcapsules in Breast Cancer." *Eur. J. Radiol.* 83 (1): 117-22.

[5] Manivasagan, P., Bui, N. Q., Bharathiraja, S., Moorthy, M. S., Oh, Y.-O., Song, K., Seo, H., Yoon, M., and Oh, J. 2017. *Multifunctional Biocompatible Chitosan-Polypyrrole Nanocomposites as Novel Agents for Photoacoustic Imaging-Guided Photothermal Ablation of Cancer.* Scientific Reports, 7.

[6] Banu, H., Sethi, D. K., Edgar, A., Sheriff, A., Rayees, N., Renuka, N., Faheem, S. M., Premkumar, K., and Vasanthakumar, G. 2015. "Doxorubicin Loaded Polymeric Gold Nanoparticles Targeted to Human Folate Receptor upon Laser Photothermal Therapy Potentiates Chemotherapy in Breast Cancer Cell Lines." *J. Photochem. Photobiol.* B149: 116-28.

[7] Salama, H., Zekri, A.-R., Zern, M., Bahnassy, A., Loutfy, S., Shalaby, S., Vigen, C., Burke, W., Mostafa, M., Alfi., O., and Medhat. E. 2010. "Autologous Hematopoietic Stem Cell Transplantation in 48 Patients with End-Stage Chronic Liver Diseases." *Cell Transplant* 19 (11): 1475-86.

[8] Youjin, J., and Kim, S. 2002. "Antitumor Activity of Chitosan Oligosaccharides Produced in Ultrafiltration Membrane Reactor System." *J Microbiol. Biotechnol.* 12: 503-7.

[9] Loutfy, S. A., El-Din, H. M. A., Elberry, M. H., Allam, N. G., Hasanin, M., and Abdellah, A. M. 2016. "Synthesis, characterization and cytotoxic evaluation of chitosan nanoparticles: in vitro liver cancer model." *Adv. Nat. Sci. Nanosci. Nanotechno.* 7 (3): 035008.

[10] Ranjha, N. M., and Khan, S. 2013. "Review Article Chitosan/Poly (vinyl Alcohol) Based Hydrogels for Biomedical Applications: A Review." *Journal of Pharmacy and Alternative Medicine (JPAM)* 2 (1): 30-41.

[11] Kracker, M., Worsch C., and Rüssel, C. 2014. "Textures of Au, Pt and Pd/PdO nanoparticles Thermally Dewetted from Thin Metal Layers on Fused Silica." *RSC Adv.* 4: 48135-43.

[12] Chen, J., Rappsilber, J., Chiang, Y.-C., Russell, P., Mann, M., and Denis, C. L. 2001. "Purification and Characterization of the 1.0 MDa CCR4-NOT Complex Identifies Two Novel Components of the Complex." *J. mol. Bio.* 314: 683-94.

[13] Zhou, Y., and Wang, W. 2010. "Study on Synergistic Effect of New Functionalized Ag Nanoparticles for Intracellular Drug Uptake in Cancer Cells." *Nano. Biomed. Eng.* 2: 208-13.

[14] AshaRani, P. V., Mun, G. L. K., Hande, M. P., and Valiyaveettil, S. 2009. "Cytotoxicity and Genotoxicity of Silver Nanoparticles in Human Cells." *ACS Nano*. 3 (2): 279-90.

[15] Osman, M. E., Eid, M. M., and Khattab, O. H. 2015. "In Vitro Cytotoxicity of Biosynthesized Ag/CS NP against MCF7, PC3 and A549 Cancer Cell Lines." *Int. J. Pharm. Tech. Res.* 8: 1011-7.

[16] Kalishwarala, K., Deepak, V., Ramkumarpandian, S., Nellaiah, H., and Sangiliyandi, G., 2008. "Extracellular Biosynthesis of Silver Nanoparticles by the Culture Supernatant of Bacillus Licheniformiss." *Mater Lett.* 62: 4411-3.

[17] Gurunathan, S., Kalishwaralal, K., Vaidyanathan, R., Deepak, V., Ram, S., Pandian, K., Muniyandi, J., Hariharan, N., and Eom, S. H. 2009. "Biosynthesis, Purification and Characterization of Silver Nanoparticles Using Escherichia Coli." *Colloids Surf.* B 74: 328-35.

[18] Sheikpranbabu, S., Kalishwaralal, K., Venkataraman, D., Eom, S. H., Park, J., and Gurunathan, S. 2009. "Silver Nanoparticles Inhibit VEGF-and IL-1β-Induced Vascular Permeability via Src Dependent Pathway in Porcine Retinal Endothelial Cells." *J. Nanobiotechnol.* 7: 8.

[19] Velmurugan, N., Kumar, G. G., Han, S. S., Nahm, K. S., and Lee, Y. S., 2009. Synthesis and characterization of potential fungicidal silver nano-sized particles and chitosan membrane containing silver particles, *Iran. Polym. J.* 18: 383-392.

[20] Vicha, V. I., and Kirtikara, K. 2006. "Sulforhodamine B Colorimetric Assay for Cytotoxicity Screening." *Nat. Protoc.* 1: 1112-6.

[21] Kanaya, T., Ohkura, M., Takeshita, H., Kaji, K., Furusaka, M., Yamaoka, H., and Wignall, G. D. 1995. "Gelation Process of Poly (Vinyl Alcohol) as Studied by Small-Angle Neutron and Light Scattering." *Macromolecules.* 28 (9): 3168-74.

[22] Kim, J., Chu, J., Shen, X., Wang, J., and Orkin, S. H. 2008. "An Extended Transcriptional Network for Pluripotency of Embryonic Stem Cells." *Cell* 132: 1049-61 .

[23] Al-Assaf, S., Coqueret, X., Haji Mohd Dahlan, K. Z., Sen, M., and Ulanski, P. 2016. "The Radiation Chemistry of

Polysaccharides." *IAEA Publications*. STI/PUB/1731. www-pub.iaea.org/MTCD/Publications/PDF/P1731_web.pdf.

[24] Ajji, Z., Othman, I., and Rosiak, J. 2005. "Production of Hydrogel Wound Dressings Using Gamma Radiation." *Nucl. Instr. Meth. Phys. Res.* B 229: 375-80.

[25] El-Hag Ali, A., Raafat, A. I. G., Mahmoud, A., Badway, N. A., El-Mottaleb, M. A., and Elshahawy, M. F. 2016. "Photocatalytic Decolorization of Dye Effluent Using Radiation Developed Polymeric Nanocomposites." *J. Inorg. Organomet. Polym. Mater.* 26: 606-15.

[26] Mansur, H. S., Costa, E. D. S., Mansur, A. A., and Barbosa-Stancioli, E. F. 2009. "Cytocompatibility Evaluation in Cell-Culture Systems of Chemically Crosslinked Chitosan/PVA Hydrogels." *Mater. Sci. Eng.* 29 (5): 1574-83.

[27] Vimala, K., Yallapu, M. M., Varaprasad, K., Reddy, N. N., Ravindra, S., Naidu, N. S., and Raju, K. M. 2011. "Fabrication of Curcumin Encapsulated Chitosan-PVA Silver Nanocomposite Films for Improved Antimicrobial Activity." *J. Biomater. Nanobiotechnol.* 2 (1): 55-64.

[28] Liu, Y., Chen, S., Zhong, L., and Wu, G. 2009. "Preparation of High-Stable Silver Nanoparticle Dispersion by Using Sodium Alginate as a Stabilizer under Gamma Radiation." *Rad. Phys. Chem.* 78: 251-5.

[29] Qi, L.-F., Xu, Z.-R., Li, Y., Jiang, X, and Han, X.-Y. 2005. "In Vitro Effects of Chitosan Nanoparticles on Proliferation of Human Gastric Carcinoma Cell Line MGC803 Cells." *World J. Gastroenterology* 11: 5136-41.

[30] Thombre, R., Mehta, S., Mohite, J., and Jaisinghani, P. 2013. "Synthesis of Silver Nanoparticles and Its Cytotoxic Effect against THP-1 Cancer Cell Line." *Int .J. Pharm. Bio. Sci.* 4: 184-92.

[31] Sriram, M. I., Kanth, S. B. M., and Kalishwaralal, K. 2010. "Antitumor Activity of Silver Nanoparticles in Dalton's Lymphoma Ascites Tumor Model." *Int. J. Nanomed.* 5: 753-62.

[32] Mansour, H., Eid, M., and El-Arnaouty, M. 2017. "Effect of Silver Nanoparticles Synthesized by Gamma Radiation on the Cytotoxicity of Doxorubicin in Human Cancer Cell Lines and Experimental Animals." *Exp. Toxicol.* doi.org/10.1177/0960327116689717 .

[33] Lanje, A. S., Sharma, S. J., and Pode, R. B. 2010. "Synthesis of Silver Nanoparticles: A Safer Alternative to Conventional Antimicrobial and Antibacterial Agents." *J. Chem. Pharm. Res.* 2: 478-83.

[34] Tiwari, D. K., Jin, T., and Ehari, J. 2011. "Dose-Dependent In-vivo Toxicity Assessment of Silver Nanoparticle in Wistar Rats." *Toxicol. Mech. Meth.* 21: 13-24.

[35] Jing, W., Ma, L., Valladares, A., Mehta, S. L., Wang, Z., Li, P. A., and Bang, J. J. 2015. "Silver Nanoparticle Exposure Induced Mitochondrial Stress, Caspase-3 Activation and Cell Death: Amelioration by Sodium Selenite." *Int. J. Biol. Sci.* 11: 860-7 .

[36] Piao, M. J., Kang, K. A., Lee, I. K., Kim, H. S., Kim, S., Choi, J. Y., Choi, J., and Hyun, J. W. 2011. "Silver Nanoparticles Induce Oxidative Cell Damage in Human Liver Cells through Inhibition of Reduced Glutathione and Induction of Mitochondria-Involved Apoptosis." *Toxicol. Lett.* 201: 92-100.

[37] El-Sherbiny, I. M., Salih, E., Yassin, A. M., and Hafez, E. E. 2016. "Newly Developed Chitosan-Silver Hybrid Nanoparticles: Biosafety and Apoptosis Induction in HepG2 Cells." *J. Nanopart. Res.* 18: 1-13 .

[38] Naghsh, N., Mashayekh, A. M., and Khodadadi, S. 2013. "Effects of Silver Nanoparticle on Lactate Dehydrogenase Activity and Histological Changes of Heart Tissue in Male Wistar Rats." *J. Fasa. Univ. Med. Sci.* 2: 303-7.

[39] Foldbjerg, R., Olesen, P., Hougaard, M., Dang, D. A., Hoffmann, H. J., and Autrup, H. 2009. "PVP-Coated Silver Nanoparticles and Silver Ions Induce Reactive Oxygen Species, Apoptosis and Necrosis in THP-1 Monocytes." *Toxicol. Lett.* 190: 156-62.

[40] Yang, E. J., Kim, S., and Kim, J. S. 2012. "Inflammasome Formation and IL-1β Release By Human Blood Monocytes in Response to Silver Nanoparticles." *Biomaterials* 33: 6858-67.

[41] Chen, C.-C., Hsieh, D.-S., Huang, K.-J., Chan, Y.-L., Hong, P.-D., Yeh, M.-K., and Wu, C.-J. 2014. "Improving Anticancer Efficacy of (–)-epigallocatechin-3-gallate Gold Nanoparticles in Murine B16F10 Melanoma Cells." *Drug Des. Devel. Ther.* 8: 459-74.

[42] Wei, L., Lu, J., Xu, H., Patel, A., Chen, Z.-S., and Chen, G. F. 2015. "Silver Nanoparticles: Synthesis, Properties, and Therapeutic Applications." *Drug Discov. Today* 20: 595-601.

[43] Guo, H., Zhang, J., Boudreau, M., Meng, J., Yin, J. J., Liu, J., and Xu, H. 2016. "Intravenous Administration of Silver Nanoparticles Causes Organ Toxicity through Intracellular ROS-Related Loss of Inter-endothelial Junction." *Part Fibre Toxicol.* 13: 1-13.